Journal of Mines, Metals and Fuels, *71(10): 1612-1619; 2023. DOI: 10.18311/jmmf/2023/35805*

Print ISSN : 0022-2755

Journal of Mines, Metals and Fuels

Contents available at: *www.informaticsjournals.com/index.php/jmmf*

Heat and Mass Transport of Casson Nanofluid in A Peristaltic Curved Channel

Gullapalli Neeraja[1], C. Kavitha[2] and A. Sreevallabha Reddy[3]

[1]Professor, Department of Mathematics, M. S. Ramaiah Institute of Technology, Bengaluru – 560054, India; neeraja.g@msrit.edu

[2]Assistance Professor, Department of Mathematics, SJRC, Bengaluru – 560009, India; ktodalbagi68@gmail.com

[3]Professor, Department of Mathematics, M. S. Ramaiah Institute of Technology, Bengaluru – 560054, India; sreevallabha@msrit.edu

Abstract

This study focuses on theoretical inquiry into transition of heat and mass of flowing Casson Nanofluid in a curved channel, in two dimensions, through peristalsis. The flow is assumed to be characterised by low Reynolds number and long wavelength approximations. The coupled governing non-dimensional equations of momentum, heat and mass transfer which are solved using BVP. Various parameters related with the flow are applied to study its effect on velocity, temperature and also nanofluid concentration. Also, the consequences of thermophoretic diffusion of nanoparticles and Brownian motion are discussed. The Casson parameter's effect on velocity profile is discussed.

Keywords: *Casson Nanofluid, Curved Channel, Peristalsis*

1.0 Introduction

Human body has always been a puzzle. It is interesting to know that passage of food through oesophagus, movement of bowels through anus, urine through bladder, etc. are involuntary actions by relaxation and contraction of muscles. This movement is known as peristalsis. This contraction and relaxation creates waves which help in propagation. Peristalsis is one of the most efficient methods employed by nature for both internal (like passage of food from oesophagus to stomach, flow of liquid from kidney to bladder, blood flow) and external (like snake movement, certain reptiles, earth worm etc.) movement.

Peristaltic fluid dynamics is of great interest to engineers and scientists because of its wide range of applications. It is used in pumping of hazardous liquid, transportation of drugs etc. Various devices like peritoneal dialysis machine, blood pumping machine, heart-lung machine etc. are designed using the principle of peristaltic transport.

Burns and Parkes[1] studied flow, with no pressure gradient under peristalsis through axially symmetric pipes and channels for viscous fluids, with small Reynolds numbers, so that Stokes flow approximations can be made. Fung and Yih[2] explored peristaltic waves in two-dimension when flow is due to movement of walls of tube in sinusoidal fashion at moderate amplitudes. The investigation was later expanded to include axisymmetric flow in a cylindrical tube. Chin-Hsiu Li[3] analyzed peristaltic pumping in a circular cylindrical tube by applying long wave approximation. It was shown that the axial pressure does not change radially in the tube. But studies were confined to Newtonian fluid where in general peristaltic transport is non-Newtonian. Researchers Srivastava and

**Author for correspondence*

Srivastava[4] looked at peristaltic transport. regarding blood, with the assumption of Reynolds number and long wavelength approximation.

Nanofluids are fluids in which minute particles are suspended. These minute particles are called as nanoparticles. The fluid in which they are suspended are base fluids. Water, ethylene, glycol, oil etc., are the base fluid. Choi *et al.*[5] were the first to study nanofluids. They studied the effect of metallic nanoparticles suspended in some fluids in order to enhance heat transfer. Akbar and Nadeem[6] studied flow of nanofluid through peristalsis in an endoscope. Sato *et al.*[7], considered flow with curved channel with a long wavelength of viscous fluid through peristalsis.

Some substances like jam, honey, mayonnaise behave like soft solids rather than fluids. Upon the application of external stress the soft solids begin to flow. Yield stress is minimum stress which activates the flow. The Casson fluid, which is non-Newtonian, is one which possesses the property of yield stress. When the applied yield stress is smaller than the shear stress, it behaves like a solid. and viscosity decrease with increase in shear rate.

B. Das *et al.*[8] studied fully developed uni-directional steady flow of a Casson fluid. Mernone *et al.*[9] studied analytically Casson fluid flow through peristalsis. Z. Abbas *et al.*[10] analysed peristaltic Casson fluid flow involving mass and energy transfer under slip conditions. The same was also studied in elliptic conduit by Salman Akhtar *et al.*[11]. Not much of literature is available regarding Casson nanofluid flow in curved channel.

The practical field of nanofluids offers a vast array of applications. The efficiency of solar thermal equipment, such as Concentrated Solar Power (CSP) plants and solar water heaters, can be increased by using nanofluids. By improving heat transmission through the use of nanofluids, receiver performance and absorption efficiency are improved, potentially lowering the number of CSP collectors required to generate power. from thermal oil as the base fluid[17]. By lowering pipeline friction, Casson nanofluids can enhance the refinery's ability to move crude oil and other fluids. These nanofluids can be effectively moved via pipelines with the help of peristalsis pumps[15]. In mining operations, peristalsis is frequently utilized to pump or convey slurry. A slurry is a mixture of liquid and solid particles. The viscosity and flow characteristics of the slurry can be enhanced by using Casson nanofluids. Mining firms can move valuable minerals or tailings from one place to another with efficiency by using peristalsis pumps to move Casson nanofluid-based slurry[16].

Hence, we intend to study flow of Casson nanofluid peristaltically in curved channel, by assuming flow to be of low Reynolds number and large wavelength approximation. Effects of different flow parameters in governing equations on velocity, temperature and nanoparticle concentration is to be analysed.

2.0 Mathematical Formulation

We consider Casson nanofluid flow in a porous curved channel, coiled as a circle of radius R with centre at O. Let 2a be the width of the channel (Figure a). Transversal deflection of sinusoidal waves creates flow of velocity $\overline{V}$. Let wall temperature and concentration be represented by T_0 and C_0 respectively, and flow pattern is given in $(\overline{r}, X, Z)$ coordinate system in laboratory frame. $\overline{r}$ is along radial direction and X being parallel to the flow direction. Z-plane is perpendicular to both $\overline{r}$ and X

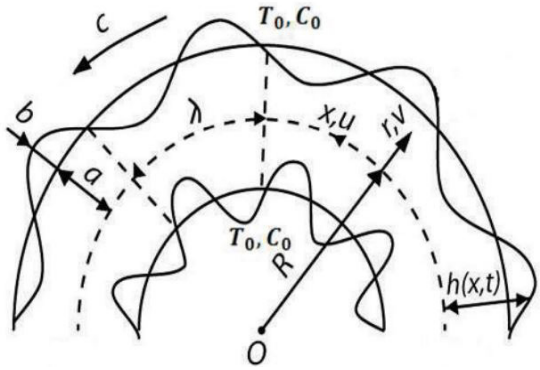

Figure a. Wave in curved channel.

planes. Let U be axial component and V be radial component of $\overline{V}$.

Equations of upper and lower walls are

$$\overline{r} = h(X,t) = a + b\sin\left(\frac{2\pi}{\lambda}(X - ct)\right) \quad (1)$$

and

$$\overline{r} = -h(X,t) = -a - b\sin\left(\frac{2\pi}{\lambda}(X - ct)\right) \quad (2)$$

where b, λ, c, , and are amplitude, wavelength, wave speed, radial displacement of upper and lower walls respectively. It is assumed that wavelength is large when compared to width of the channel, i.e. $\frac{a}{\lambda} \le 1$. Casson fluid model stress tensor[12,13] is given by

$$\bar{\tau} = \begin{cases} \left(\mu_b + \frac{P_y}{\sqrt{2\pi}}\right)\bar{A}, if\ \pi > \pi_c \\ \left(\mu_b + \frac{P_y}{\sqrt{2\pi_c}}\right)\bar{A}, if\ \pi < \pi_c \end{cases} \quad (3)$$

where μ_b, P_y, and π_c are plastic dynamic viscosity, yield stress and critical value respectively and π is the second invariant of A.

Here $\bar{A} = grad\,\bar{V} + \left(grad\,\bar{V}\right)^T$ (4)

and $P_y = \frac{\mu_b\sqrt{2\pi_c}}{\beta}$ (5)

β is Casson material parameter

For $\pi > \pi_c$, $\mu = \mu_b + \frac{P_y}{\sqrt{2\pi_c}}$ (6)

Therefore from (3),

$$\bar{\tau} = \mu_b\left(1 + \frac{1}{\beta}\right)\bar{A} \quad (7)$$

Equations governing the flow are

Continuity equation

$$\frac{\partial\left(\bar{r}+R\right)V}{\partial\bar{r}} + R\frac{\partial U}{\partial X} = 0$$

i.e. $$\frac{\partial V}{\partial\bar{r}} + \frac{V}{\bar{r}+R} + \frac{R}{\bar{r}+R}\frac{\partial U}{\partial X} = 0 \quad (8)$$

Momentum equation in radial direction

$$\rho_f\left[\frac{\partial V}{\partial t} + \left(\bar{V}\cdot\nabla\right)V - \frac{U^2}{\bar{r}+R}\right] = -\frac{\partial P}{\partial\bar{r}} + \mu_b\left(1+\frac{1}{\beta}\right)\left[\nabla^2 V - \frac{V}{\left(\bar{r}+R\right)^2} - \frac{2R}{\left(\bar{r}+R\right)^2}\frac{\partial U}{\partial X}\right] - \frac{\nu}{k^*}V$$

i.e.

$$\rho_f\left[\frac{\partial V}{\partial t} + \frac{RU}{\bar{r}+R}\frac{\partial V}{\partial X} + V\frac{\partial V}{\partial\bar{r}} - \frac{U^2}{\bar{r}+R}\right] = -\frac{\partial P}{\partial\bar{r}} +$$

$$\mu_b\left(1+\frac{1}{\beta}\right)\left[\left(\frac{R}{\bar{r}+R}\right)^2\frac{\partial^2 V}{\partial X^2} + \frac{1}{\bar{r}+R}\frac{\partial V}{\partial\bar{r}} + \right.$$

$$\left. + \frac{\partial^2 V}{\partial\bar{r}^2} - \frac{V}{\left(\bar{r}+R\right)^2} - \frac{2R}{\left(\bar{r}+R\right)^2}\frac{\partial U}{\partial X}\right] - \frac{\nu}{k^*}V \quad (9)$$

Momentum equation in axial direction

$$\rho_f\left[\frac{\partial U}{\partial t} + \frac{RU}{\bar{r}+R}\frac{\partial U}{\partial X} + V\frac{\partial U}{\partial\bar{r}} + \frac{UV}{\bar{r}+R}\right] = -\frac{R}{\bar{r}+R}\frac{\partial P}{\partial X}$$

$$+\mu_b\left(1+\frac{1}{\beta}\right)\left[\left\{\left(\frac{R}{\bar{r}+R}\right)^2\frac{\partial^2 V}{\partial X^2} + \frac{1}{\bar{r}+R}\frac{\partial U}{\partial\bar{r}} + \frac{\partial^2 U}{\partial\bar{r}^2}\right\}\right.$$

$$\left. - \frac{U}{\left(\bar{r}+R\right)^2} + \frac{2R}{\left(\bar{r}+R\right)^2}\frac{\partial V}{\partial X}\right] - \frac{\nu}{k^*}U + \left[\left(1-C_0\right)\rho_f g\beta_T\left(T-T_0\right) +$$

$$\left(\rho_p - \rho_f\right)g\beta_C\left(C-C_0\right)\ \right] \quad (10)$$

Energy conservation equation

i.e.

$$\frac{\partial T}{\partial\bar{t}} + \frac{RU}{\bar{r}+R}\frac{\partial T}{\partial X} + V\frac{\partial T}{\partial\bar{r}} = \frac{k}{(\rho c)_p}\left[\left(\frac{R}{\bar{r}+R}\right)^2\frac{\partial^2 T}{\partial X^2} + \frac{1}{\bar{r}+R}\frac{\partial T}{\partial\bar{r}} + \frac{\partial^2 T}{\partial\bar{r}^2}\right] +$$

$$\gamma\left[D_B\left(\nabla C\cdot\nabla T\right) + \frac{D_T}{T_m}\left(\nabla T\cdot\nabla T\right)\right] + \frac{\mu}{(\rho c)_p}\left[4\left(\frac{\partial V}{\partial\bar{r}}\right)^2 + \left(\frac{\partial U}{\partial\bar{r}} + \frac{U}{\bar{r}+R} + \frac{\partial V}{\partial X}\right)^2\right] \quad (11)$$

Nanoparticle concentration equation

$$\frac{\partial C}{\partial\bar{t}} + \left(\bar{V}\cdot\nabla\right)C = D_B\nabla^2 C + \frac{D_T}{T_m}\nabla^2 T$$

i.e.

$$\frac{\partial C}{\partial\bar{t}} + \frac{RU}{\bar{r}+R}\frac{\partial C}{\partial X} + V\frac{\partial C}{\partial\bar{r}} = D_B\left[\left(\frac{R}{\bar{r}+R}\right)^2\frac{\partial^2 C}{\partial X^2} + \frac{1}{\bar{r}+R}\frac{\partial C}{\partial\bar{r}} + \frac{\partial^2 C}{\partial\bar{r}^2}\right] +$$

$$\frac{D_T}{T_m}\left[\left(\frac{R}{\bar{r}+R}\right)^2\frac{\partial^2 T}{\partial X^2} + + \frac{1}{\bar{r}+R}\frac{\partial T}{\partial\bar{r}} + \frac{\partial^2 T}{\partial\bar{r}^2}\right] \quad (12)$$

where

$$P,\ C,\ T,\ g,\ \rho_f,\ \rho_p,\ \mu,\ \nu,\ k,\ k^*,\ c_p,\ \gamma = \frac{(\rho c)_p}{(\rho c)_f},\ \beta_T,\ \beta_c,\ D_B,\ D_T,\ T_m$$

represent pressure, concentration, temperature, acceleration due to gravity, base fluid density, nanoparticle density, dynamic viscosity, kinematic viscosity, thermal conductivity, permeability of porous medium, specific heat, ratio of heat capacity of nanoparticle to heat capacity of fluid, coefficient of linear thermal expansion, coefficient of expansion with concentration, Brownian diffusion

coefficient, thermophoretic coefficient and mean temperature respectively.

The following transformations are employed to shift laboratory frame $(\bar{r}, X)$ to wave frame (r, x),

$$x = X - ct, r = \bar{r}, p = P, v = V, u = U - c, T = T$$

Then (8)-(12) gets transformed to equations given below

$$\frac{\partial v}{\partial r} + \frac{v}{r+R} + \frac{R}{r+R}\frac{\partial u}{\partial x} = 0 \tag{13}$$

$$\rho_f\left[\frac{\partial v}{\partial t} + \frac{R(u+c)}{r+R}\frac{\partial v}{\partial x} + v\frac{\partial v}{\partial r} - \frac{(u+c)^2}{r+R}\right] = -\frac{\partial p}{\partial r} + \mu_b\left(1+\frac{1}{\beta}\right)\left[\left(\frac{R}{r+R}\right)^2\frac{\partial^2 v}{\partial x^2} + \frac{1}{r+R}\frac{\partial v}{\partial r} + \frac{\partial^2 v}{\partial r^2} - \frac{v}{(r+R)^2} - \frac{2R}{(r+R)^2}\frac{\partial u}{\partial x}\right] - \frac{v}{k^*}v \tag{14}$$

$$\rho_f\left[\frac{\partial u}{\partial t} + \frac{R(u+c)}{r+R}\frac{\partial u}{\partial x} + v\frac{\partial u}{\partial r} + \frac{(u+c)v}{r+R}\right] = -\frac{R}{r+R}\frac{\partial p}{\partial x} + \mu_b\left(1+\frac{1}{\beta}\right)\left[\left\{\left(\frac{R}{r+R}\right)^2\frac{\partial^2 v}{\partial x^2} + \frac{1}{r+R}\frac{\partial u}{\partial r} + \frac{\partial^2 u}{\partial r^2}\right\} - \frac{u+c}{(r+R)^2} + \frac{2R}{(r+R)^2}\frac{\partial v}{\partial x}\right] - \frac{v}{k^*}(u+c) + \left[(1-C_0)\rho_f g\beta_T(T-T_0) + (\rho_p - \rho_f)g\beta_C(C-C_0)\right] \tag{15}$$

$$\frac{\partial T}{\partial t} + \frac{R(u+c)}{r+R}\frac{\partial T}{\partial x} + v\frac{\partial T}{\partial r} = \frac{k}{(\rho c)_p}\left[\left(\frac{R}{r+R}\right)^2\frac{\partial^2 T}{\partial x^2} + \frac{1}{r+R}\frac{\partial T}{\partial r} + \frac{\partial^2 T}{\partial r^2}\right] + \gamma\left[D_B\frac{\partial C}{\partial r}\cdot\frac{\partial T}{\partial r} + \frac{D_T}{D_m}\left(\frac{\partial T}{\partial r}\right)^2\right] + \frac{\mu}{(\rho c)_p}\left[4\left(\frac{\partial v}{\partial r}\right)^2 + \left(\frac{\partial u}{\partial r} + \frac{u+c}{r+R} + \frac{\partial v}{\partial x}\right)^2\right] \tag{16}$$

$$\frac{\partial C}{\partial t} + \frac{Ru}{r+R}\frac{\partial C}{\partial x} + v\frac{\partial C}{\partial r} = D\left[\left(\frac{R}{r+R}\right)\frac{\partial^2 C}{\partial x^2} + \frac{\partial C}{r+R\,\partial r} + \frac{\partial^2 C}{\partial r^2}\right] + \frac{}{T}\left[\left(\frac{R}{r+R}\right)\frac{\partial^2 T}{\partial x^2} + \frac{\partial T}{r+R\,\partial r} + \frac{\partial^2 T}{\partial r^2}\right] \tag{17}$$

Introducing variables which are non-dimensional

$$x' = \frac{x}{\lambda}, r' = \frac{r}{a}, u' = \frac{u}{c}, v' = \frac{v}{\delta c}, \delta = \frac{a}{\lambda}, t' = \frac{ct}{\lambda}, \phi = \frac{b}{a}, k' = \frac{R}{a}, p' = \frac{a^2 p}{\mu c\lambda},$$

$$F = \frac{Q}{ac}, \sigma = \frac{C-C_0}{C_0}, \theta = \frac{T-T_0}{T_0}, P_r = \frac{\mu c_p}{k}, E_c = \frac{c^2}{c_p T_0}, N_B = \frac{\gamma D_B C_0}{\nu}, N_T = \frac{\gamma D_T T_0}{T_m \nu},$$

$$R_e = \frac{\rho_f ca}{\mu}, G_r = \frac{(1-C_0)\beta_T g T_0 a^2}{c\nu}, G_c = \frac{(\rho_p - \rho_f)\beta_C g C_0 a^2}{c\mu}, D = \frac{a^2\nu}{\mu k^*}$$

where $\delta, \phi, k', R_e, P_r, E_c, N_B, N_t, G_r, G_c$ are wave number, amplitude ratio, curvature parameter, Reynolds number, Prandtl number, Eckert number, Brownian motion parameter, thermophoresis parameter, local temperature Grashof number and local nanoparticle Grashof number respectively.

Dropping primes and introducing stream function, following V.K. Narla *et al.*[14], $u = -\frac{\partial \psi}{\partial r}, v = \frac{\delta k'}{r+k'}\frac{\partial \psi}{\partial x}$ applying the dimensionless quantities and using the assumption that the flow is of low Reynolds number and long wavelength approximation and eliminating pressure factor, (13) is identically satisfied and (14) - (17) becomes

$$\left(1+\frac{1}{\beta}\right)\left[-\frac{2}{k'}\frac{\partial^3\psi}{\partial r^3} - \frac{r+k'}{k'}\frac{\partial^4\psi}{\partial r^4} + \frac{-\frac{\partial\psi}{\partial r}+1}{k'(r+k')^2} + \frac{1}{k'(r+k')}\frac{\partial^2\psi}{\partial r^2}\right] - \frac{1}{k'}\left(-\frac{\partial\psi}{\partial r}+1\right) + \frac{r+k'}{k'}\frac{\partial^2\psi}{\partial r^2} + \left[\frac{G_r\theta}{k'} + G_r\frac{r+k'}{k'}\frac{\partial\theta}{\partial r} + \frac{G_c\sigma}{k'} + G_c\frac{r+k'}{k'}\frac{\partial\sigma}{\partial r}\right] = 0 \tag{18}$$

$$\left[\frac{1}{r+k'}\frac{\partial\theta}{\partial r} + \frac{\partial^2\theta}{\partial r^2}\right] + P_r N_B\frac{\partial\theta}{\partial r}\frac{\partial\sigma}{\partial r} + P_r N_T\left(\frac{\partial\theta}{\partial r}\right)^2 + P_r E_c\left(\frac{\partial u}{\partial r} + \frac{-\frac{\partial\psi}{\partial r}+1}{r+k'}\right) = 0 \tag{19}$$

$$\left[\frac{1}{r+k'}\frac{\partial\sigma}{\partial r} + \frac{\partial^2\sigma}{\partial r^2}\right] + \frac{N_T}{N_B}\left[\frac{1}{r+k'}\frac{\partial\theta}{\partial r} + \frac{\partial^2\theta}{\partial r^2}\right] = 0 \tag{20}$$

The boundary conditions are taken

$$\psi = \pm\frac{F}{2}, \frac{\partial\psi}{\partial r} = 0, \theta = 0, \sigma = 0, at\ r = \pm\left(1+\phi\sin(2\pi x)\right)$$

3.0 Results and Discussion

The coupled non-linear differential equations (18)-(20), with the boundary conditions, are solved for velocity, temperature, and concentration of nanoparticle, by using MATLAB package.

Through this article we study the impact of various factors like curvature k', Casson fluid parameter β, local temperature Grashof number G_r, local nanoparticle Grashof number G_c, Brownian motion parameter N_B, thermophorosis parameter N_T, on fluid velocity u, temperature distribution θ and nanoparticle concentration σ.

From figure 1 it can be observed that as the value of curvature k' decreases velocity profile u increases and the maximum velocity is about the central line $r=0$, since small curvature makes the channel straight. In this case fluid flows faster along the centre of the channel. When k' large, flow is towards the lower wall. When Casson parameter β increases value of yield stresses P_y decreases and vice-versa. With decreasing value of P_y there is decrease in velocity profile u. But decrease in velocity is halted due to thermal conductivity. From figure 2 it can be observed that flow is towards the lower wall, as viscosity increases. When β decreases velocity profile u increases because of increase in yield stress and u attains maximum about the central line $r=0$. Increase in Grashof number G_r implies dominance of buoyancy force over viscous force. Figure 3 shows that velocity profile u increases towards the lower wall and when G_r decreases viscous force dominates buoyancy force. Hence u decrease. As local nanoparticle Grashof number G_c decreases Figure 4 says velocity profile u decreases towards the lower wall because of concentration of nanoparticles towards the lower wall and velocity profile u increases towards the upper side of wall when G_c increases, due to increase in buoyancy. As Brownian motion parameter N_B increases velocity profile u increases towards lower wall, because of increase in random movement of particles. Also, since N_B is inversely proportional to viscosity. As N_B decreases, u also decreases, because viscosity increases, as is shown in Figure 5. If thermophorosis parameter N_T increases velocity profile u also increases towards upper wall, due to increase in nanoparticles, which in turn increases

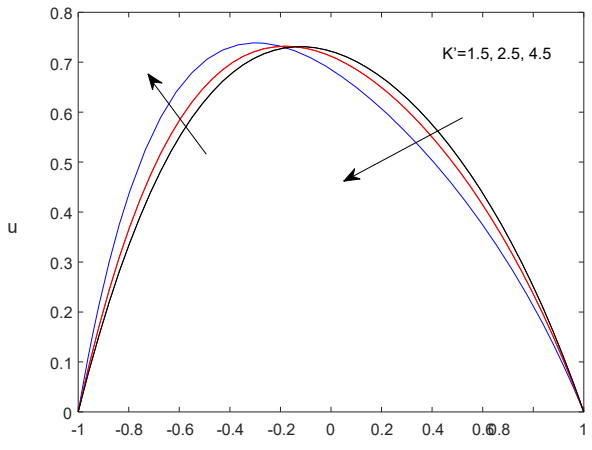

Figure 1. . The effect of curvature k' on velocity.

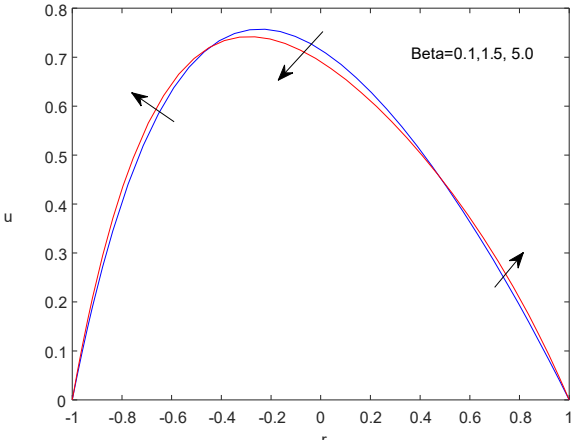

Figure 2. Effect of Casson parameter β on velocity u.

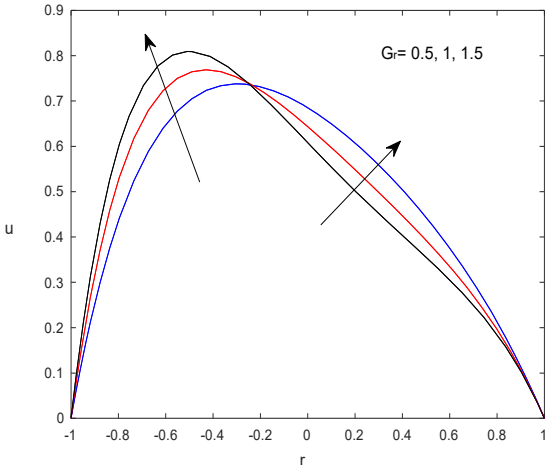

Figure 3. Effect of local temperature Grashof Number on velocity.

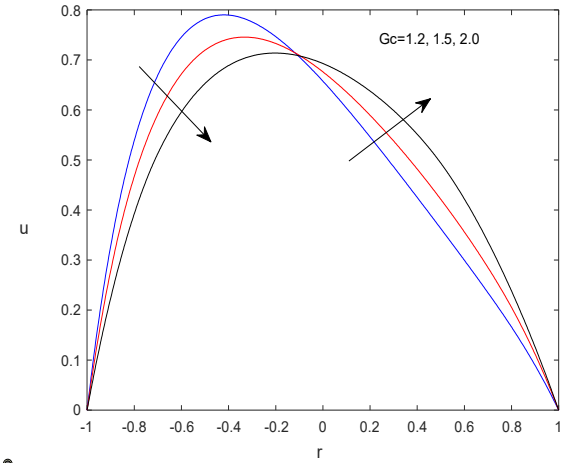

Figure 4. Effect of local nano particle Grashof Number on velocity.

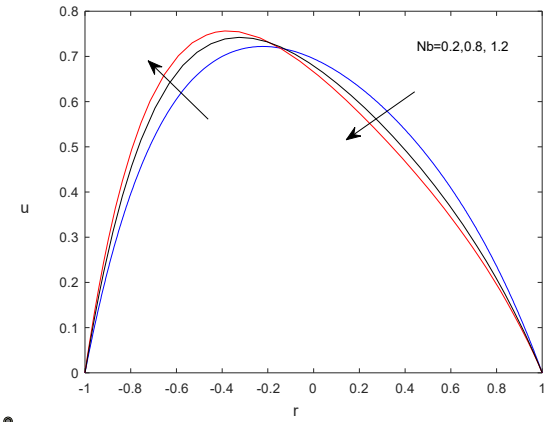

Figure 5. Effect of Brownian motion parameter on velocity.

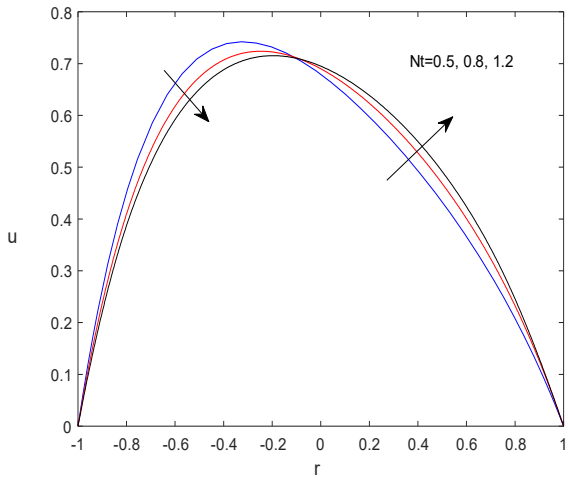

Figure 6. Effect of Thermoporosis parameter on velocity.

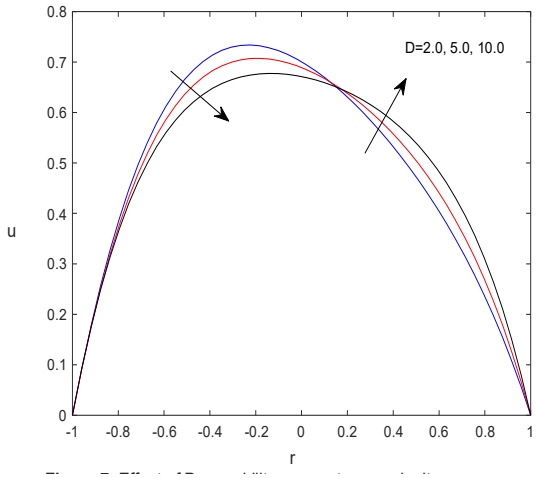

Figure 7. Effect of Permeability parameter on velocity.

collision of particles. Figure 6 shows that as N_T decreases u also decrease towards lower wall. Due to porosity of the channel, as the permeability parameter D increases, the velocity profile u increases around $r = 0$ of the channel. This is shown in figure 7.

Local temperature Grashof number G_r, and local nanoparticle Grashof number G_c has same effect on temperature θ. As seen in Figures 8 and 9, increase in the value of G_r and G_c increases the temperature θ due to natural convection. Also due to the fact that G_r and G_c are inversely proportional to viscosity and temperature reaches its peak towards the upper wall. Figure 10 shows that as Brownian motion parameter N_B decreases temperature θ decreases, because reduction in N_B reduces collision of particles, which reduces nanoparticle

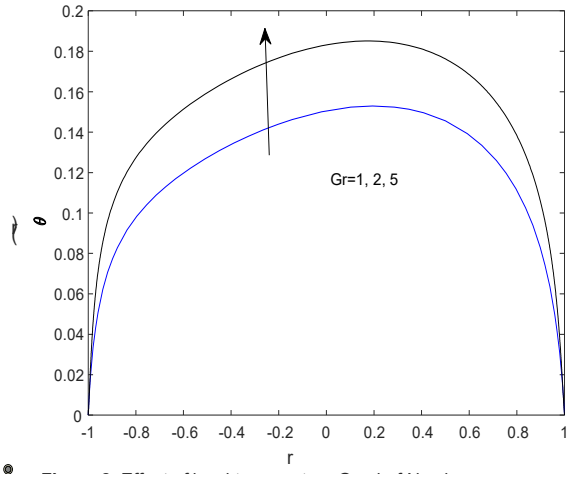

Figure 8. Effect of local temperature Grashof Number on temperature.

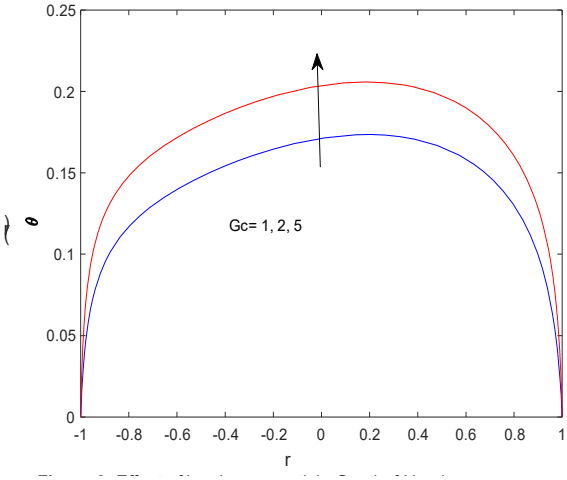

Figure 9. Effect of local nano particle Grashof Number on temperature.

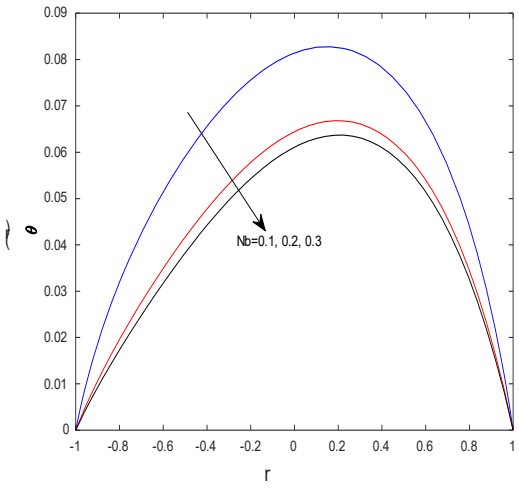

Figure 10. Effect of Brownian motion parameter on temperature.

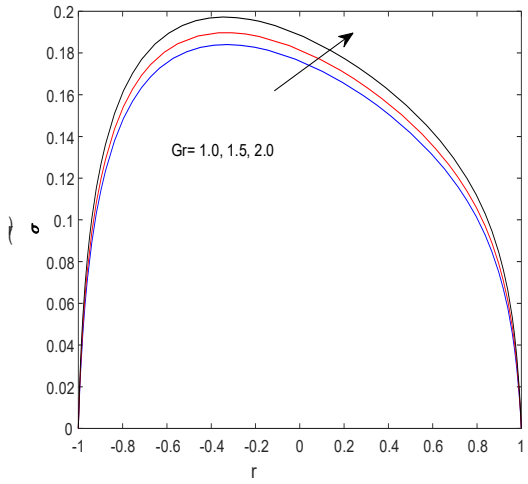

Figure 12. Effect of local temperature Grashof Number on

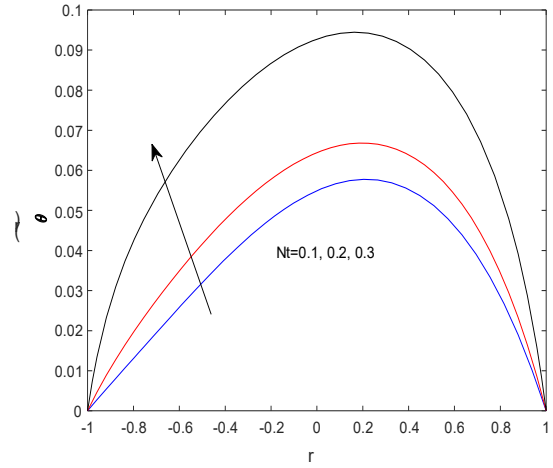

Figure 11. Effect of Thermophoresis parameter on temperature.

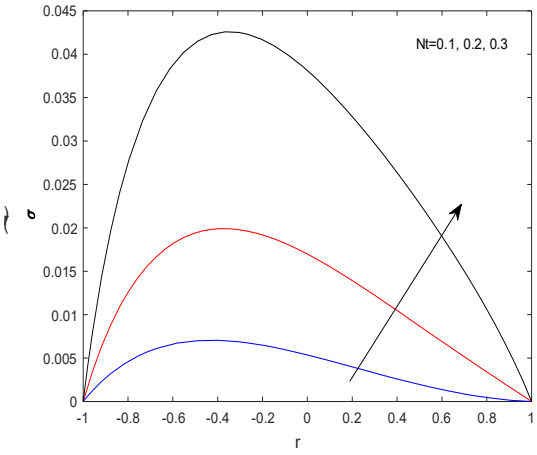

Figure 13. Effect of Thermoporosis parameter on concentration.

temperature. Temperature reaches its peak around the central line $r = 0$. With the increase in thermophorosis parameter N_T, heat transfer rate increases on the surface. Figure 11 shows that temperature reaches its peak around the central line $r = 0$. Increasing value of Local temperature Grashof number G_r increases buoyancy force over viscous force, hence concentration σ reaches peak towards the lower wall and decrease towards the upper wall. This is depicted in Figure 12. Increase in thermophorosis parameter N_T increases the concentration.

4.0 Concluding Remarks

The transition of heat and mass in a curved channel of Casson nanofluid is the subject of study in this paper. in a curved channel, in two dimensions, through peristalsis, under the assumption that the flow is characterised by low Reynolds number and long wavelength approximations. The coupled governing non-dimensional equations of momentum, heat and mass transfer are solved using MATLAB package. The effects of various parameters on

velocity, temperature and nanofluid concentration are studied. It was observed that

- As the curvature k' decreases velocity profile u increases and the maximum velocity is about the central line $r = 0$.
- When Casson parameter β decreases velocity profile u increases because of increase in yield stress and u attains maximum about the central line $r = 0$.
- When Grashof number G_r decreases viscous force dominates buoyancy force. Hence u decrease.
- Velocity profile u increases towards the upper side of wall when local nanoparticle Grashof number G_c increases, due to increase in buoyancy.
- As Brownian motion parameter N_B and thermophorosis parameter N_T increases velocity profile also u increases towards lower wall, because of increase in random movement of particles.
- Increase in the values of Local temperature Grashof number G_r and local nanoparticle Grashof number G_c increases the temperature θ due to natural convection.

5.0 References

1. Burns JC and Parkes T. Peristaltic motion. *Journal of Fluid Mechanics.* 1967; 29(4):731-743.
2. Fung YC, Yih CS. Peristaltic Transport. *Journal of Applied Mechanics.* 1968; 35(4):669-675.
3. Chin-Hsiu L, Peristaltic transport in circular cylindrical tubes. *Journal of Biomechanics.* 1970; 3(5):513-523.
4. Srivastava LM, Srivastava VP. Peristaltic transport of blood: Casson model—II. J Biomech. 1984; 17(11): 821-9.
5. Choi SU, Eastman JA. Enhancing Thermal Conductivity of fluids with nanoparticles. ASME FED- 1995. 231/ MD-Vol. 66:99–105.
6. Akbar, Nadeem. Endoscopic Effects on Peristaltic Flow of a Nanofluid. Commun Theor Phys. 2011; 56(4):761.
7. Sato H, Kawai T, Fujita T, Okabe M. Two-Dimensional Peristaltic Flow in Curved Channels. Trans Jpn Soc Mech Eng. 2000; 66(643):679-685.
8. Das B, Batra RL. Secondary flow of a Casson fluid in a slightly curved tube. Int J Non-Linear Mech. 1993; 28(5):567-577.
9. Mernone AV, Mazumdar JN, Lucas SK. A Mathematical Study of Peristaltic Transport of a Casson Fluid. Math Comput Model. 2002; 35:895-912.
10. Abbas Z, Rafiq MY, Hasnain J, Javed T. Peristaltic Transport of a Casson Fluid in a Non-uniform Inclined Tube with Rosseland Approximation and Wall Properties. Arab J Sci Eng. 2020; 46(3).
11. Akhtara S, Almutairib S, Nadeema S. Impact of heat and mass transfer on the Peristaltic flow of non-Newtonian Casson fluid inside an elliptic conduit: Exact solutions through novel technique. Chin J Phys. 2022; 78:194-206.
12. Farooq S, Hayat T, Ahmad B. A Theoretical Analysis for Peristalsis of Casson Material with Thermal Radiation and Viscous Dissipation. Thermal Sci. 2019; 23(6A):3351-3364.
13. Ahmed R, Ali N, Khan S, Chamkha A, Tlili I. Heat and mass transfer characteristics in flow of bi-viscosity fluid through a curved channel with contracting and expanding walls: A finite difference approach. Adv Mech Eng. 2020; 12(10):1–16.
14. Narla VK, Prasad KM, Ramanamurthy JV. Peristaltic Transport of Jeffrey NanoFluid in Curved Channels. Procedia Eng. 2015; 127:869-876.
15. Akbar NS. Influence of magnetic field on peristaltic flow of a Casson fluid in an asymmetric channel: Application in crude oil refinement. J Magn Magn Mater. 2014.
16. Asha SK, Namrata K. Thermal analysis for peristaltic flow of nanofluid under the influence of porous medium and double diffusion in a non-uniform channel using Sumudu Transformation Method. Ann Pure Appl Math. 2021; 23(2):73-91.
17. Sami S. Analysis of Nanofluids Behaviour in Concentrated Solar Power Collectors with Organic Rankine Cycle. Appl Syst Innov. 2019; 2(3):22.